NBDT: NEURAL-BACKED DECISION TREE

Anonymous authors
Paper under double-blind review

ABSTRACT

Machine learning applications such as finance and medicine demand accurate and justifiable predictions, barring most deep learning methods from use. In response, previous work combines decision trees with deep learning, yielding models that (1) sacrifice interpretability for accuracy or (2) sacrifice accuracy for interpretability. We forgo this dilemma by *jointly improving* accuracy and interpretability using Neural-Backed Decision Trees (NBDTs). NBDTs replace a neural network's final linear layer with a differentiable sequence of decisions and a surrogate loss. This forces the model to learn high-level concepts and lessens reliance on highly-uncertain decisions, yielding (1) accuracy: NBDTs match or outperform modern neural networks on CIFAR, ImageNet and better generalize to unseen classes by up to 16%. Furthermore, our surrogate loss improves the *original* model's accuracy by up to 2%. NBDTs also afford (2) interpretability: visual evidence of generalization, uncovering ambiguous ImageNet labels, and improving human trust.

1 INTRODUCTION

Many computer vision applications (*e.g.* medical imaging and autonomous driving) require insight into the model's decision process, complicating applications of deep learning which are traditionally black box. Recent efforts in explainable computer vision attempt to address this need and can be grouped into one of two categories: (1) saliency maps and (2) sequential decision processes.

Saliency maps retroactively explain model predictions by identifying which pixels most affected the prediction. However, by focusing on the input, saliency maps fail to capture the model's decision making process. For example, saliency offers no insight for a misclassification when the model is "looking" at the right object for the wrong reasons. Alternatively, we can gain insight into the model's decision process by breaking up predictions into a sequence of smaller semantically meaningful decisions as in rule-based models like decision trees. However, existing efforts to fuse deep learning and decision trees suffer from (1) significant accuracy loss, relative to contemporary models (e.g., residual networks), (2) reduced interpretability due to accuracy optimizations (e.g., impure leaves and ensembles), and (3) tree structures that offer limited insight into the model's credibility.

To address these, we propose **Neural-Backed Decision Trees (NBDTs)** to jointly improve *both* (1) accuracy and (2) interpretability of modern neural networks, utilizing decision rules that preserve (3) properties like sequential, discrete decisions; pure leaves; and non-ensembled predictions. These properties in unison enable unique insights, as we show. To accomplish this, NBDTs replace the final linear layer of a neural network with a differentiable oblique decision tree and, unlike its predecessors (*i.e.* decision trees, hierarchical classifiers), uses a hierarchy derived from model parameters, does not employ a hierarchical softmax, and can be created from *any* existing classification neural network without architectural modifications. These improvements tailor the hierarchy to the network rather than overfit to the feature space, lessens the decision tree's reliance on highly uncertain decisions, and encourages accurate recognition of high-level concepts. These benefits culminate in joint improvement of accuracy and interpretability. Our contributions are as follows:

1. We propose a *tree supervision loss*, yielding NBDTs that match/outperform and outgeneralize modern neural networks (WideResNet, EfficientNet) on ImageNet, TinyImageNet200, and CIFAR100. Our loss also improves the *original* model by up to 2%.
2. We propose alternative hierarchies for oblique decision trees – *induced hierarchies* built using neural network weights – that outperform both data-based hierarchies (*e.g.* built with information gain) and existing hierarchies (*e.g.* WordNet), in accuracy.

3. We show visual evidence of each decision rule's interpretability and leverage insights uniquely afforded by this hierarchy to present qualitative evidence of generalization, find ambiguous ImageNet labels, and improve human trust.

2 Related Works

Saliency maps. Numerous efforts (Springenberg et al., 2014; Zeiler & Fergus, 2014; Simonyan et al., 2013; Zhang et al., 2016; Selvaraju et al., 2017; Ribeiro et al., 2016; Petsiuk et al., 2018; Sundararajan et al., 2017) have explored the design of saliency maps identifying pixels that most influenced the model's prediction. White-box techniques (Springenberg et al., 2014; Zeiler & Fergus, 2014; Simonyan et al., 2013; Selvaraju et al., 2017; Sundararajan et al., 2017) use the network's parameters to determine salient image regions, and black-box techniques (Ribeiro et al., 2016; Petsiuk et al., 2018) determine pixel importance by measuring the prediction's response to perturbed inputs. However, saliency does not explain the model's decision process (*e.g.* Was the model confused early on, distinguishing between *Animal* and *Vehicle*? Or is it only confused between dog breeds?).

Transfer to Explainable Models. Prior to the recent success of deep learning, decision trees were state-of-the-art on a wide variety of learning tasks and the gold standard for interpretability. Despite this recency, study at the intersection of neural network and decision tree dates back three decades, where neural networks were seeded with decision tree weights (Banerjee, 1990; 1994; Ivanova & Kubat, 1995a;b), and decision trees were created from neural network queries (Krishnan et al., 1999; Boz, 2000; Dancey et al., 2004; Craven & Shavlik, 1996; 1994), like distillation (Hinton et al., 2015). The modern analog of both sets of work (Humbird et al., 2018; Siu, 2019; Frosst & Hinton, 2017) evaluate on feature-sparse, sample-sparse regimes such as the UCI datasets (Dua & Graff, 2017) or MNIST (LeCun et al., 2010) and *perform poorly* on standard image classification tasks.

Hybrid Models. Recent work produces hybrid decision tree and neural network models to scale up to datasets like CIFAR10 (Krizhevsky, 2009), CIFAR100 (Krizhevsky, 2009), TinyImageNet (Le & Yang, 2015), and ImageNet (Deng et al., 2009). One category of models organizes the neural network into a hierarchy, dynamically selecting branches to run inference (Veit & Belongie, 2018; McGill & Perona, 2017; Teja Mullapudi et al., 2018; Redmon & Farhadi, 2017; Murdock et al., 2016). However, these models use *impure leaves* resulting in uninterpretatble, stochastic paths. Other approaches fuse deep learning into each decision tree node: an entire neural network (Murthy et al., 2016), several layers (Murdock et al., 2016; Roy & Todorovic, 2016), a linear layer (Ahmed et al., 2016), or some other parameterization of neural network output (Kontschieder et al., 2015). These models likewise limit interpretability by supporting no more than depth-2 trees (Ahmed et al., 2016; Guo et al., 2018) or employing an ensemble (Kontschieder et al., 2015; Ahmed et al., 2016), where ensembles are often referred to as "black boxes" (Carvalho et al., 2019; Rudin, 2018).

Hierarchical Classification (Silla & Freitas, 2011). One set of approaches directly uses a pre-existing hierarchy over classes, such as WordNet (Redmon & Farhadi, 2017; Brust & Denzler, 2019; Deng et al.). However *conceptual similarity is not indicative of visual similarity*. Other models build a hierarchy using the training set directly, via a classic data-dependent metric like Gini impurity (Alaniz & Akata, 2019) or information gain (Rota Bulo & Kontschieder, 2014; Biçici et al., 2018). These models are instead *prone to overfitting*, per (Tanno et al., 2019). Finally, several works introduce hierarchical surrogate losses (Wu et al., 2017; Deng et al., 2012), such as hierarchical softmax (Mohammed & Umaashankar, 2018), but as the authors note, these methods quickly suffer from major accuracy loss with more classes or higher-resolution images (*e.g.* beyond CIFAR10). We demonstrate hierarchical classifiers attain higher accuracy *without* a hierarchical softmax.

3 Method

Neural-Backed Decision Trees (NBDTs) replace a network's final linear layer with a decision tree. Unlike previous decision trees or hierarchical classifiers, NBDTs use path probabilities for inference (Sec 3.1) to devalue high-entropy decisions, build a hierarchy from model weights (Sec 3.2) to lessen overfitting, and train with a hierarchical loss (Sec 3.3) to better represent high-level concepts.

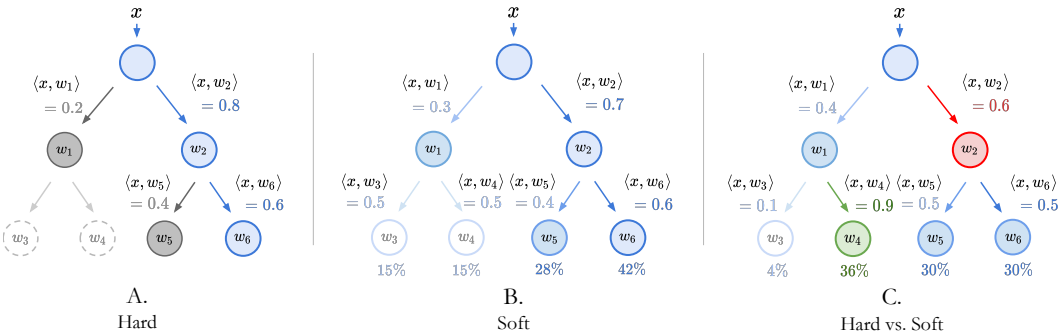

Figure 1: Hard and Soft Decision Trees. A. Hard: is the classic "hard" oblique decision tree. Each node picks the child node with the largest inner product, and visits that node next. Continue until a leaf is reached. **B. Soft:** is the "soft" variant, where each node simply returns probabilities, as normalized inner products, of each child. For each leaf, compute the probability of its path to the root. Pick leaf with the highest probability. **C. Hard vs. Soft:** Assume w_4 is the correct class. With hard inference, the mistake at the root (red) is irrecoverable. However, with soft inference, the highly-uncertain decisions at the root and at w_2 are superseded by the highly certain decision at w_3 (green). This means the model can still correctly pick w_4 despite a mistake at the root. In short, soft inference can tolerate mistakes in highly uncertain decisions.

3.1 Inference

Our NBDT first featurizes each sample using the neural network backbone; the backbone consists of all neural network layers before the final linear layer. Second, we run the final fully-connected layer as an oblique decision tree. However, (a) a classic decision tree cannot recover from a mistake early in the hierarchy and (b) just running a classic decision tree on neural features drops accuracy significantly, by up to 11% (Table 2). Thus, we present modified decision rules (Figure 1, B):

1. Seed oblique decision rule weights with neural network weights. An oblique decision tree defines a hyperplane for each decision rule and thus only supports binary decision. Instead, we associate a "representative" vector r_i with each node. For each leaf's representative, use a row vector $r_i = w_i$, which represents a class, from the fully-connected layer weights W. For each inner node's representative, use the average of its leave's representatives $r_i = \frac{1}{n}\sum_{i=1}^{n} w_i$.

2. Compute node probabilities. For each sample x and node i, compute the probability of each child $j \in C(i)$ using $p(j|i) = \textsc{Softmax}(\langle \vec{r}_i, x\rangle)[j]$, where $\vec{r}_i = (\langle r_k, x\rangle)_{k \in C(i)}$.

3. Pick a leaf using path probabilities. Inspired by Deng et al. (2012), consider a leaf ℓ and its path from the root P_ℓ. The probability of each node $i \in P_\ell$ traversing the next node in the path $C_\ell(i) \in P_\ell \cap C(i)$ is denoted $p(C_\ell(i)|i)$. Then, the probability of leaf ℓ and its class c is

$$p(c) = p(\ell) = \Pi_{i \in P_\ell} p(C_\ell(i)|i) \tag{1}$$

In soft inference, the final class prediction $\hat{c}$ is defined over these class probabilities,

$$\hat{c} = \text{argmax}_c p(c) = \text{argmax}_\ell \Pi_{i \in P_\ell} p(C_\ell(i)|i) \tag{2}$$

Our inference strategy has two benefits: (a) Since the architecture is unchanged, the fully-connected layer can be run regularly (Table 4) or as sequential decision rules (Table 1), and (b) unlike decision trees and other conditionally-executed models (Tanno et al., 2019; Veit & Belongie, 2018), our method can recover from a mistake early in the hierarchy with sufficient uncertainty in the incorrect path (Figure 1 C, Appendix Table 6) This inference mode bests classic tree inference (Appendix C).

3.2 Building Induced Hierarchies

Existing decision-tree-based methods use (a) hierarchies built with data-dependent heuristics like information gain or (b) existing hierarchies like WordNet. However, the former overfits to the data, and the latter focuses on conceptual rather than visual similarity: For example, by virtue of being an

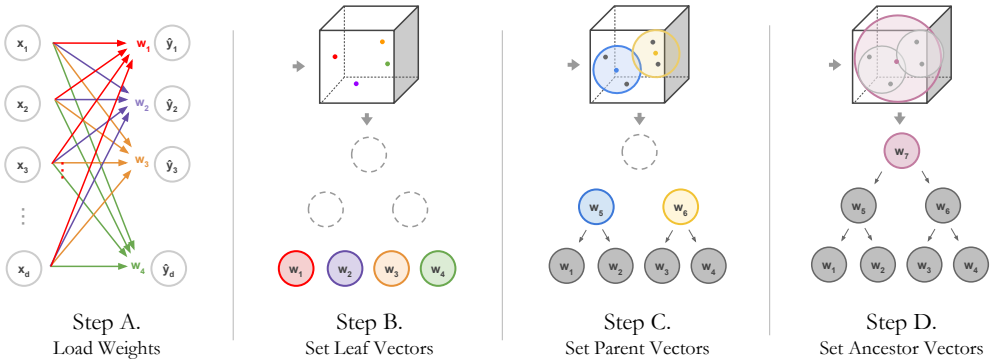

Figure 2: Building Induced Hierarchies. Step A. Load the weights of pre-trained neural network's final fully-connected layer, with weight matrix $W \in \mathbb{R}^{d \times k}$. **Step B.** Use each row w_i of W as representative vectors for each leaf node. For example, the red w_1 from A is assigned to the red leaf in B. **Step C.** Use the average of each pair of leaves for the parents' representative vectors. For example, w_1 and w_2 (red and purple) in B are averaged to make w_5 (blue) in C. **Step D.** For each ancestor, take the subtree it is the root for. Average representative vectors for all leaves in the subtree. That average is the ancestor's representative vector. In this figure, the ancestor is the root, so its representative vector is the average of all leaves w_1, w_2, w_3, w_4.

animal, *Bird* is closer to *Cat* than to *Plane*, according to WordNet. However, the opposite is true for visual similarity: by virtue of being in the sky, *Bird* is more visually similar to *Plane* than to *Cat*. Thus, to prevent overfitting and reflect visual similarity, we build a hierarchy using model weights.

In particular, we take row vectors w_i, each representing a class, from the fully-connected layer weights W. Then, we run hierarchical agglomerative clustering on the class representatives w_i. Each leaf is represented by a vector w_i (Figure 2, Step B) and each inner node's r_i is the average of its leave's representatives (Figure 2, Step C). We refer to this hierarchy as the *induced hierarchy* (Figure 2).

3.3 Training with Tree Supervision Loss

Even though standard cross entropy loss separates representatives for each leaf, it is not trained to separate representatives for each inner node (Table 3, "None"). To amend this, we add a *tree supervision loss*, a cross entropy loss over the class distribution of path probabilities $\mathcal{D}_{\text{nbdt}} = \{p(c)\}_{c=1}^{\mathcal{C}}$ (Eq. 1) from Sec 3.1, with time-varying weights ω_t, β_t:

$$\mathcal{L} = \beta_t \underbrace{\text{CrossEntropy}(\mathcal{D}_{\text{pred}}, \mathcal{D}_{\text{label}})}_{\mathcal{L}_{\text{original}}} + \omega_t \underbrace{\text{CrossEntropy}(\mathcal{D}_{\text{nbdt}}, \mathcal{D}_{\text{label}})}_{\mathcal{L}_{\text{soft}}} \tag{3}$$

Note that (a) tree supervision loss damages learning speed early in training, when leaf and thus inner node representatives are nonsensical. Thus, our tree supervision weight ω_t grows from 0 to $\omega_T = 0.5$ for CIFAR10, CIFAR100, and to $\omega_T = 5$ for TinyImageNet, ImageNet. The hyperparameter $\beta_t \in [0, 1]$ decays over time. (b) We re-train where possible, fine-tuning with $\mathcal{L}_{\text{soft}}$ only when the original model accuracy is not reproducible. (c) Unlike hierarchical softmax, our path-probability cross entropy loss $\mathcal{L}_{\text{soft}}$ disproportionately up-weights decisions earlier in the hierarchy, encouraging accurate high-level decisions; this is reflected our out-generalization of the baseline neural network by up to 16% to unseen classes (Table 5).

4 Experiments

NBDTs obtain state-of-the-art results for interpretable models and match or outperform modern neural networks on image classification. We report results on different models (ResNet, WideResNet, EfficientNet) and datasets (CIFAR10, CIFAR100, TinyImageNet, ImageNet). We additionally conduct ablation studies to verify the hierarchy and loss designs, find that our training procedure

Table 1: Results. NBDT outperforms competing decision-tree-based methods by up to 18% and can also outperform the *original* neural network by $\sim$ 1%. "Expl?" indicates the method retains interpretable properties: pure leaves, sequential decisions, non-ensemble. Methods without this check see reduced interpretability. We bold the highest decision-tree-based accuracy. We use reported results or improve them using a stronger backbone: DNDF (Kontschieder et al., 2015), XOC (Alaniz & Akata, 2019), DCDJ (Baek et al., 2017), NofE (Ahmed et al., 2016), DDN (Murthy et al., 2016), ANT (Tanno et al., 2019), CNN-RNN (Guo et al., 2018).

Method	Backbone	Expl?	CIFAR10	CIFAR100	TinyImageNet
NN	WideResNet28x10	✗	*97.62%*	*82.09%*	*67.65%*
ANT-A*	*n/a*	✓	93.28%	*n/a*	*n/a*
DDN	NiN	✗	90.32%	68.35%	*n/a*
DCDJ	NiN	✗	*n/a*	69.0%	*n/a*
NofE	ResNet56-4x	✗	*n/a*	76.24%	*n/a*
CNN-RNN	WideResNet28x10	✓	*n/a*	76.23%	*n/a*
NBDT-S (Ours)	WideResNet28x10	✓	**97.55%**	**82.97%**	**67.72%**
NN	ResNet18	✗	*94.97%*	*75.92%*	*64.13%*
DNDF	ResNet18	✗	94.32%	67.18%	44.56%
XOC	ResNet18	✓	93.12%	*n/a*	*n/a*
DT	ResNet18	✓	93.97%	64.45%	52.09%
NBDT-S (Ours)	ResNet18	✓	**94.82%**	**77.09%**	**64.23%**

Figure 3: ImageNet Results. NBDT outperforms all competing decision-tree-based methods by at least 14%, staying within 0.6% of EfficientNet accuracy. "Explainable?" indicates the method retains interpretable properties. Methods without this check see reduced interpretability. "EfficientNet" is EfficientNet-EdgeTPU-Small.

	NN	NofE	XOC	NBDT-S (Ours)
Explainable?	✗	✗	✓	✓
Backbone	EfficientNet	AlexNet	ResNet152	EfficientNet
ImageNet	*77.23%*	61.29%	60.77%	**76.60%**

improves the *original* neural network's accuracy by up to 2%, and show that NBDTs improve generalization to unseen classes by up to 16%. All reported improvements are absolute.

4.1 Results

Small-scale Datasets. Our method (Table 1) matches or outperforms recently state-of-the-art neural networks. On CIFAR10 and TinyImageNet, NBDT accuracy falls within 0.15% of the baseline neural network. On CIFAR100, NBDT accuracy outperforms the baseline by $\sim$1%.

Large-scale Dataset. On ImageNet (Table 3), NBDTs obtain 76.60% top-1 accuracy, outperforming the strongest competitor NofE by 15%. Note that we take the best competing results for any decision-tree-based method, but the strongest competitors hinder interpretability by using ensembles of models like a decision forest (DNDF, DCDJ) or feature shallow trees with only depth 2 (NofE).

4.2 Analysis

Hierarchy Ablation. Table 2 shows that our induced hierarchies outperform alternatives. In particular, *data-dependent* hierarchies overfit, and the existing *WordNet hierarchy* focuses on conceptual rather than visual similarity.

Loss Ablation. Previous work suggests a hierarchical softmax (Appendix B) is necessary for a hierarchical classifier. However, our results suggest otherwise: NBDTs trained with hierarchical softmax instead of tree supervision loss see a $\sim$3% drop in accuracy on TinyImageNet (Table 3).

Original Neural Network. Per Sec 3.1, we can run the original neural network's fully-connected layer normally, after training with tree supervision loss. Using this, we find that the original neural network's accuracy improves by up to 2% on CIFAR100, TinyImageNet (Table 4).

Table 2: Comparisons of Hierarchies. We demonstrate that our weight-space hierarchy bests taxonomy and data-dependent hierarchies. In particular, the induced hierarchy achieves better performance than (a) the WordNet hierarchy, (b) a classic decision tree's information gain hierarchy, built over neural features ("Info Gain"), and (c) an oblique decision tree built over neural features ("OC1").

Dataset	Backbone	Original	Induced	Info Gain	WordNet	OC1
CIFAR10	ResNet18	*94.97%*	**94.82%**	93.97%	94.37%	94.33%
CIFAR100	ResNet18	*75.92%*	**77.09%**	64.45%	74.08%	38.67%
TinyImageNet200	ResNet18	*64.13%*	**64.23%**	52.09%	60.26%	15.63%

Table 3: Comparisons of Losses. Training the NBDT using tree supervision loss with a linearly increasing weight ("TreeSup(t)") is superior to training (a) with a constant-weight tree supervision loss ("TreeSup"), (b) with a hierarchical softmax ("HrchSmax") and (c) without extra loss terms. ("None"). Δ is the accuracy difference between our soft loss and hierarchical softmax.

Dataset	Backbone	Original	TreeSup(t)	TreeSup	None	HrchSmax
CIFAR10	ResNet18	*94.97%*	**94.82%**	97.57%	94.38%	93.97%
CIFAR100	ResNet18	*75.92%*	**77.09%**	74.92%	61.93%	74.09%
TinyImageNet200	ResNet18	*64.13%*	**64.23%**	62.74%	45.51%	61.12%

Zero-Shot Superclass Generalization. We define a "superclass" to be the hypernym of several classes. (*e.g. Animal* is a superclass of *Cat* and *Dog*). Using WordNet (per Sec 3.2), we (1) identify which superclasses each NBDT inner node is deciding between (*e.g. Animal vs. Vehicle*). (2) We find unseen classes that belong to the same superclass, from a different dataset. (*e.g.* Pull *Turtle* images from ImageNet). (3) Evaluate the model to ensure the unseen class is classified into the correct superclass (*e.g.* ensure *Turtle* is classified as *Animal*). For an NBDT, this is straightforward: one of the inner nodes classifies *Animal vs. Vehicle* (Sec 5.1). For a standard neural network, we consider the superclass that the final prediction belongs to. (*i.e.* When evaluating *Animal vs. Vehicle* on a *Turtle* image, the CIFAR-trained model may predict any CIFAR *Animal* class). See Appendix A.1 for details. Our NBDT consistently bests the original neural network by 8%+ (Table 5). When discerning *Carnivore vs. Ungulate*, NBDT outperforms the original neural network by 16%.

5 INTERPRETABILITY

The interpretability of a decision tree is well-established when input features are easily understood (*e.g.* tabular data in medicine or finance). However, when the input is more complex like neural features, this becomes more challenging. Fortunately, previous work shows these neural features are visually interpretable (Olah et al., 2017). As a result, we focus on *how* these features are used. Specifically, we show several interpretable insights unique to our hierarchical classifier, which are unattainable with a standard linear layer: NBDTs are able to (a) learn more generalized representations of high level concepts (eg. *Animal*) (Sec 5.2), (b) identify ImageNet samples with ambiguous

Dataset	Backbone	NN	NN-S
C100	R18	75.92%	**76.96%**
T200	R18	64.13%	**66.55%**
C100	WRN28	82.09%	**82.87%**
T200	WRN28	67.65%	**68.51%**

Table 4: Original Neural Network. We compare the model's accuracy before and after the tree supervision loss, using ResNet18, WideResNet on CIFAR100, TinyImageNet. Our loss increases the original network accuracy consistently by $\sim .8 - 2.4\%$. NN-S is the network trained with the tree supervision loss.

n_{class}	Superclasses	R18	NBDT-S
71	Animal *vs.* Vehicle	66.08%	**74.79%**
36	Placental *vs.* Vertebrate	45.50%	**54.89%**
19	Carnivore *vs.* Ungulate	51.37%	**67.78%**
9	Motor Vehicle *vs.* Craft	69.33%	**77.78%**

Table 5: Zero-Shot Superclass Generalization. We evaluate a CIFAR10-trained NBDT (ResNet18 backbone) inner node's ability to generalize beyond seen classes. We label TinyImageNet with superclass labels (*e.g.* label *Dog* with *Animal*) and evaluate nodes distinguishing between said superclasses. We compare to the baseline ResNet18: check if the prediction is within the right superclass.

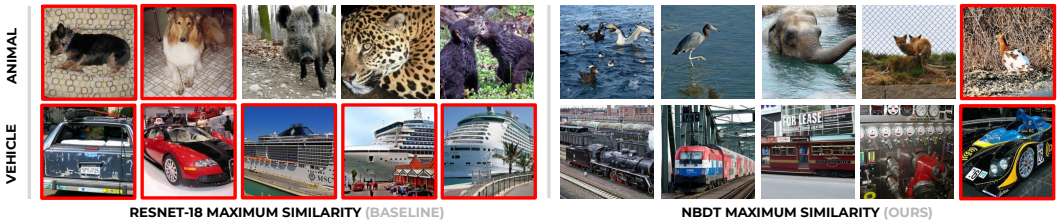

Figure 4: Maximum Similarity Examples. We run two CIFAR10-trained models, one trained with tree supervision loss (NBDT) and one without (ResNet18). We compute the induced hierarchy of both models and find samples most similar to the *Animal*, and *Motor Vehicle* concepts. Each row represents an inner node, and the red borders indicate images that contain CIFAR10 classes. (1) Note that NBDT's concept of an animal includes classes and contexts it was not trained on; aquatic animals (top-right) and trains (bottom-right) are not a part of CIFAR10. In contrast, ResNet18 largely finds examples closely related to existing CIFAR10 classes (dog, car, boat). This is qualitative evidence that NBDTs better generalize.

labels (Sec 5.3), and (c) improve human trust, especially for misclassified images (Sec 5.4). Note that these analyses depend on three model properties that NBDT preserves: (1) discrete, sequential decisions, so that one path is selected; (2) pure leaves, so that one path picks one class; and (3) non-ensembled predictions, so that path to prediction attribution is discrete.

5.1 Labeling Decision Nodes

WordNet provides interpretable labels for hierarchies with leaves corresponding to nouns, like in ours. However, the WordNet corpus is lacking in (a) object attributes and (b) abstract visual ideas (*e.g.* , context) that are not themselves objects, like "cylindrical body", "blue background" or "red" – many of which are littered across our induced hierarchies (Appendix Figure 13). Despite this limitation, we use WordNet to assign meaning to intermediate decision nodes, with more sophisticated methods left to future work: For any node, consider all leaves it is an ancestor of, and compute the earliest WordNet ancestor of all these leaves. This ancestor is used as the WordNet meaning. We then use these hypothesized WordNet meanings for the subsequent analyses.

5.2 Maximum Similarity Examples to Visualize Generalization

We (1) visually confirm the hypothesized meaning of each node by identifying the most "representative" samples, and (2) check that these "representative" samples represent that category (*e.g.* , *Animal*) and not just the training classes under that category. We define "representative" samples, or maximum similarity examples, to be samples with embeddings most similar to an inner node's representative. We visualize these examples for a model before and after the tree supervision loss (NBDT and ResNet18, respectively). The models are trained on CIFAR10, but samples are drawn from ImageNet. We observe that maximum similarity examples for NBDT contain more unseen classes than ResNet18 (Figure 4). This suggests that our NBDT is better able to capture high-level concepts such as *Animal*, which is quantitatively confirmed by the superclass evaluation in Table 5.

5.3 Path Entropy for Dataset Debugging

There are several types of ambiguous labels (Figure 5), any of which could hurt model performance for an image classification dataset like ImageNet. To find these images, we use entropy in NBDT decisions, which we find is a much stronger indicator of ambiguity than entropy in the original neural network prediction. The intuition is as follows: If all intermediate decisions have high certainty except for a few decisions, those decisions are deciding between multiple equally plausible cases. Using this intuition, we can identify ambiguous labels by finding samples with high "path entropy" – or highly disparate entropies for intermediate decisions on the NBDT prediction path.

Per Figure 6, the highest "path entropy" samples in ImageNet contain multiple objects, where each object could plausibly be used for the image class. In contrast, samples that induce the highest entropy in the baseline neural network do not suggest ambiguous labels. This suggests NBDT entropy is more informative compared to that of a standard neural network.

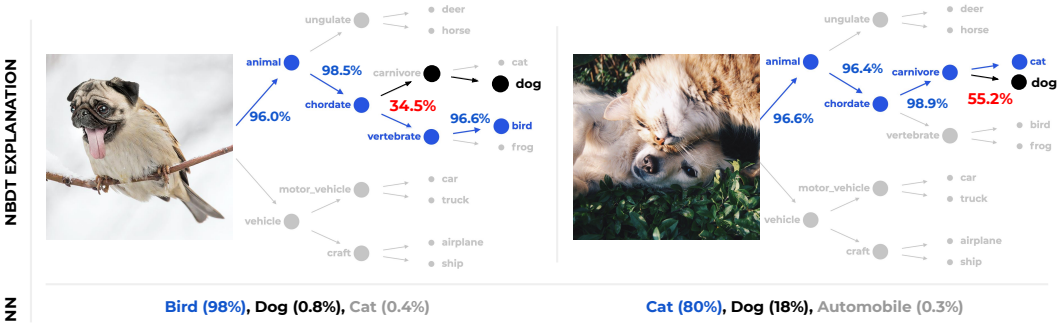

Figure 5: Types of Ambiguous Labels. All these examples have ambiguous labels. With NBDT (top), the decision rule deciding between equally-plausible classes has low certainty (red, 30-50%). All other decision rules have high certainty (blue, 96%+). The juxtaposition of high and low certainty decision rules makes ambiguous labels easy to distinguish. By contrast, ResNet18 (bottom) still picks one class with high probability. (Left) An extreme example of a "spug" that may plausibly belong to two classes. (Right) Image containing two animals of different classes. Photo ownership: "Spug" by Arne Fredriksen at gyyporama.com. Used with permission. Second image is CC-0 licensed at pexels.com.

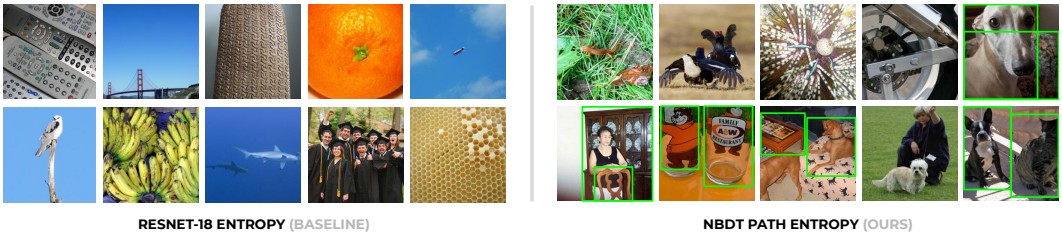

Figure 6: ImageNet Ambiguous Labels. These images suggest that NBDT path entropy uniquely identifies ambiguous labels in Imagenet, without object detection labels. We plot ImageNet validation samples that induce the most 2-class confusion, using TinyImagenet200-trained models. Note that ImageNet classes do not include people. (Left) Run ResNet18 and find samples that (a) maximize entropy between the top 2 classes and (b) minimize entropy across all classes, where the top 2 classes are averaged. Despite high model uncertainty, half the classes are from the training set – bee, orange, bridge, banana, remote control – and do not show visual ambiguity. (Right) For NBDT, compute entropy for each node's predicted distribution; take the difference between the largest and smallest values. Now, half of the images contain truly ambiguous content for a classifier; we draw green boxes around pairs of objects that could each plausibly be used for the image class.

5.4 Path Traversal for Improved Human Trust

The explanation of an NBDT prediction is the visualization of the path traversed. We then compare these NBDT explanations to other explainability methods in human studies. Specifically, we ask participants to pick an expert to trust (Appendix, Figure 12), based on the expert's explanation – a saliency map (ResNet18, GradCAM), a decision tree (NBDT), or neither. We only use samples where ResNet18 and NBDT predictions agree. Of 374 respondents that picked one method over the other, **65.9%** prefer NBDT explanations; for misclassified samples, **73.5%** prefer NBDT. This suggests that humans trust NBDTs more than current saliency techniques.

6 Conclusion

In this work, we propose Neural-Backed Decision Trees that see (1) improved accuracy: NBDTs out-generalize (16%+), improve (2%+), and match (0.15%) or outperform (1%+) state-of-the-art neural networks on CIFAR10, CIFAR100, TinyImageNet, and ImageNet. We also show (2) improved interpretability by drawing unique insights from our hierarchy, showing visual evidence of generalizability, ambiguous ImageNet labels, and improved human trust. This challenges the conventional supposition of a dichotomy between accuracy and interpretability, paving the way for jointly accurate *and* interpretable models in real-world deployments.

REFERENCES

Karim Ahmed, Mohammadharis Baig, and Lorenzo Torresani. Network of experts for large-scale image categorization. volume 9911, April 2016.

Stephan Alaniz and Zeynep Akata. XOC: explainable observer-classifier for explainable binary decisions. *CoRR*, abs/1902.01780, 2019.

Seungryul Baek, Kwang In Kim, and Tae-Kyun Kim. Deep convolutional decision jungle for image classification. *CoRR*, abs/1706.02003, 2017.

Arunava Banerjee. Initializing neural networks using decision trees. 1990.

Arunava Banerjee. Initializing neural networks using decision trees. In *Proceedings of the International Workshop on Computational Learning and Natural Learning Systems*, pp. 3–15. MIT Press, 1994.

Ufuk Can Biçici, Cem Keskin, and Lale Akarun. Conditional information gain networks. In *2018 24th International Conference on Pattern Recognition (ICPR)*, pp. 1390–1395. IEEE, 2018.

Olcay Boz. Converting a trained neural network to a decision tree dectext - decision tree extractor. In *ICMLA*, 2000.

Clemens-Alexander Brust and Joachim Denzler. Integrating domain knowledge: using hierarchies to improve deep classifiers. In *Asian Conference on Pattern Recognition*, pp. 3–16. Springer, 2019.

Diogo V Carvalho, Eduardo M Pereira, and Jaime S Cardoso. Machine learning interpretability: A survey on methods and metrics. *Electronics*, 8(8):832, 2019.

Mark Craven and Jude W Shavlik. Extracting tree-structured representations of trained networks. In *Advances in neural information processing systems*, pp. 24–30, 1996.

Mark W Craven and Jude W Shavlik. Using sampling and queries to extract rules from trained neural networks. In *Machine learning proceedings 1994*, pp. 37–45. Elsevier, 1994.

Darren Dancey, David McLean, and Zuhair Bandar. Decision tree extraction from trained neural networks. January 2004.

J. Deng, W. Dong, R. Socher, L.-J. Li, K. Li, and L. Fei-Fei. ImageNet: A Large-Scale Hierarchical Image Database. In *CVPR09*, 2009.

Jia Deng, Nan Ding, Yangqing Jia, Andrea Frome, Kevin Murphy, Samy Bengio, Yuan Li, Hartmut Neven, and Hartwig Adam. Large-scale object classification using label relation graphs.

Jia Deng, Jonathan Krause, Alexander C Berg, and Li Fei-Fei. Hedging your bets: Optimizing accuracy-specificity trade-offs in large scale visual recognition. In *2012 IEEE Conference on Computer Vision and Pattern Recognition*, pp. 3450–3457. IEEE, 2012.

Dheeru Dua and Casey Graff. UCI machine learning repository, 2017. URL http://archive.ics.uci.edu/ml.

Nicholas Frosst and Geoffrey E. Hinton. Distilling a neural network into a soft decision tree. *CoRR*, abs/1711.09784, 2017.

Yanming Guo, Yu Liu, Erwin M Bakker, Yuanhao Guo, and Michael S Lew. Cnn-rnn: a large-scale hierarchical image classification framework. *Multimedia Tools and Applications*, 77(8):10251–10271, 2018.

Geoffrey Hinton, Oriol Vinyals, and Jeff Dean. Distilling the knowledge in a neural network. *arXiv preprint arXiv:1503.02531*, 2015.

Kelli Humbird, Luc Peterson, and Ryan McClarren. Deep neural network initialization with decision trees. *IEEE Transactions on Neural Networks and Learning Systems*, PP:1–10, October 2018.

Irena Ivanova and Miroslav Kubat. Initialization of neural networks by means of decision trees. *Knowledge-Based Systems*, 8(6):333 – 344, 1995a. Knowledge-based neural networks.

Irena Ivanova and Miroslav Kubat. Decision-tree based neural network (extended abstract). In *Machine Learning: ECML-95*, pp. 295–298, Berlin, Heidelberg, 1995b. Springer Berlin Heidelberg.

Peter Kontschieder, Madalina Fiterau, Antonio Criminisi, and Samuel Rota Bulo. Deep neural decision forests. In *The IEEE International Conference on Computer Vision (ICCV)*, December 2015.

R. Krishnan, G. Sivakumar, and P. Bhattacharya. Extracting decision trees from trained neural networks. *Pattern Recognition*, 32(12):1999 – 2009, 1999.

Alex Krizhevsky. Learning multiple layers of features from tiny images. Technical report, 2009.

Ya Le and Xuan Yang. Tiny imagenet visual recognition challenge. 2015.

Yann LeCun, Corinna Cortes, and CJ Burges. Mnist handwritten digit database. *ATT Labs [Online]. Available: http://yann. lecun. com/exdb/mnist*, 2, 2010.

Mason McGill and Pietro Perona. Deciding how to decide: Dynamic routing in artificial neural networks. In *ICML*, 2017.

Abdul Arfat Mohammed and Venkatesh Umaashankar. Effectiveness of hierarchical softmax in large scale classification tasks. In *2018 International Conference on Advances in Computing, Communications and Informatics (ICACCI)*, pp. 1090–1094. IEEE, 2018.

Calvin Murdock, Zhen Li, Howard Zhou, and Tom Duerig. Blockout: Dynamic model selection for hierarchical deep networks. In *Proceedings of the IEEE conference on computer vision and pattern recognition*, pp. 2583–2591, 2016.

Venkatesh N. Murthy, Vivek Singh, Terrence Chen, R. Manmatha, and Dorin Comaniciu. Deep decision network for multi-class image classification. In *The IEEE Conference on Computer Vision and Pattern Recognition (CVPR)*, June 2016.

Chris Olah, Alexander Mordvintsev, and Ludwig Schubert. Feature visualization. *Distill*, 2017. doi: 10.23915/distill.00007. https://distill.pub/2017/feature-visualization.

Vitali Petsiuk, Abir Das, and Kate Saenko. Rise: Randomized input sampling for explanation of black-box models. In *Proceedings of the British Machine Vision Conference (BMVC)*, 2018.

Joseph Redmon and Ali Farhadi. Yolo9000: better, faster, stronger. In *Proceedings of the IEEE conference on computer vision and pattern recognition*, pp. 7263–7271, 2017.

Marco Tulio Ribeiro, Sameer Singh, and Carlos Guestrin. "why should I trust you?": Explaining the predictions of any classifier. In *Proceedings of the 22nd ACM SIGKDD International Conference on Knowledge Discovery and Data Mining, San Francisco, CA, USA, August 13-17, 2016*, pp. 1135–1144, 2016.

Samuel Rota Bulo and Peter Kontschieder. Neural decision forests for semantic image labelling. In *Proceedings of the IEEE Conference on Computer Vision and Pattern Recognition*, pp. 81–88, 2014.

Anirban Roy and Sinisa Todorovic. Monocular depth estimation using neural regression forest. In *Proceedings of the IEEE conference on computer vision and pattern recognition*, pp. 5506–5514, 2016.

C Rudin. Stop explaining black box machine learning models for high stakes decisions and use interpretable models instead. manuscript based on c. rudin please stop explaining black box machine learning models for high stakes decisions. In *Proceedings of NeurIPS 2018 Workshop on Critiquing and Correcting Trends in Learning*, 2018.

Ramprasaath R Selvaraju, Michael Cogswell, Abhishek Das, Ramakrishna Vedantam, Devi Parikh, and Dhruv Batra. Grad-cam: Visual explanations from deep networks via gradient-based localization. In *IEEE Conference on Computer Vision and Pattern Recognition (CVPR)*, pp. 618–626, 2017.

Carlos N Silla and Alex A Freitas. A survey of hierarchical classification across different application domains. *Data Mining and Knowledge Discovery*, 22(1-2):31–72, 2011.

Karen Simonyan, Andrea Vedaldi, and Andrew Zisserman. Deep inside convolutional networks: Visualising image classification models and saliency maps. *arXiv preprint arXiv:1312.6034*, 2013.

Chapman Siu. Transferring tree ensembles to neural networks. In *Neural Information Processing*, pp. 471–480, 2019.

Jost Tobias Springenberg, Alexey Dosovitskiy, Thomas Brox, and Martin A. Riedmiller. Striving for simplicity: The all convolutional net. *CoRR*, abs/1412.6806, 2014.

Mukund Sundararajan, Ankur Taly, and Qiqi Yan. Axiomatic attribution for deep networks. *International Conference on Machine Learning (ICML) 2017*, 2017.

Ryutaro Tanno, Kai Arulkumaran, Daniel C. Alexander, Antonio Criminisi, and Aditya Nori. Adaptive neural trees, 2019.

Ravi Teja Mullapudi, William R. Mark, Noam Shazeer, and Kayvon Fatahalian. Hydranets: Specialized dynamic architectures for efficient inference. In *The IEEE Conference on Computer Vision and Pattern Recognition (CVPR)*, June 2018.

Andreas Veit and Serge Belongie. Convolutional networks with adaptive inference graphs. In *The European Conference on Computer Vision (ECCV)*, September 2018.

Mike Wu, M Hughes, Sonali Parbhoo, and F Doshi-Velez. Beyond sparsity: Tree-based regularization of deep models for interpretability. In *In: Neural Information Processing Systems (NIPS) Conference. Transparent and Interpretable Machine Learning in Safety Critical Environments (TIML) Workshop*, 2017.

Matthew D Zeiler and Rob Fergus. Visualizing and understanding convolutional networks. In *European Conference on Computer Vision (ECCV)*, pp. 818–833. Springer, 2014.

Jianming Zhang, Zhe Lin, Jonathan Brandt, Xiaohui Shen, and Stan Sclaroff. Top-down neural attention by excitation backprop. In *European Conference on Computer Vision (ECCV)*, pp. 543–559. Springer, 2016.